CERN-ACC-NOTE-2018-0029

2018-03-27

rmargraf@stanford.edu

Muon Beam Studies in the H4 beam line and the Gamma Irradiation Facility (GIF++)

R. Margraf[1,2,3] and N. Charitonidis[2]*

Keywords: Beam Line Simulations, H4 Beam Line, Gamma Irradiation Facility, GOLIATH

Abstract

In this note, we present detailed simulation results for the trajectory of a muon beam, traversing beam zones PPE-134 and PPE-154, produced by a 150 GeV positive hadron beam incident on collimators 9 & 10 in the H4 beam line when these collimators are placed off-beam axis to stop all hadrons and electrons. Using G4Beamline, a GEANT-4 based Monte-Carlo program, the trajectory of the muon beam has been studied for several field strengths of the GOLIATH magnet, as well as for different polarities. The position of the beam at the Gamma Irradiation Facility (GIF++), located downstream the PPE-144 area, is also presented. In addition, two configurations of the two XTDV's present in the line (XTDV.022.520 and XTDV.022.610) have been studied, with the purpose to simulate the pion contamination of the beam both in PPE134 and GIF++.

*Corresponding Author
[1]Lehigh University, Bethlehem, PA, United States
[2]CERN, Geneva, Switzerland
[3]Stanford University, Stanford, CA, United States

Contents

1 Introduction

1.1 The North Area H4 beam line and GIF++

The H4 beam line, located in CERN's EHN1 facility, is a multi-purpose beam line capable of transporting secondary or tertiary particle beams, produced on the T2 primary target, over a very wide momentum range, from 10 GeV/c up to 400 GeV/c [1]. These secondary particles are transported to three experimental areas ("zones"), PPE-134, GIF++ (PPE-154), and the CMS reserved zone (PPE-164). An additional zone, PPE-144, is located between PPE-134 and GIF++. The PPE-134 area is an experimental zone used by several test-beams for R&D of detectors or detector components [2]. Moreover, it hosts the GOLIATH magnet, a large horizontal dipole magnet with maximum design strength of 1.5T, used as an experimental spectrometer. As with every electromagnet, GOLIATH's polarity can be also be reversed to produce a field in the opposite direction.

The GIF++ facility is located directly downstream of PPE-144, and offers to its users the possibility to test detector components or experimental equipment exposed simultaneously to gamma photons (produced by a strong Cs source) and charged particle beams (mostly muons of a few hundreds of GeV).

A muon beam can be produced by incidence of a pion-rich beam on many nuclear interaction lengths of material, stopping all hadrons and electrons and letting through only muons from pion and kaon decays. The most convenient way to produce this kind of beam is using the line's collimators located upstream of the GOLIATH magnet. A double, 4-jaw collimator, designated "Collimator 9" for the horizontal plane and "Collimator 10," for the vertical, acts in most cases as this pion dump. When functioning as a dump, the jaws of Collimators 9 and 10 are set in a position offset from the nominal beam axis. The total length of iron in the beam direction is in this case equal to 1 m.

The produced muon beam can be used by users in both the PPE-134 and GIF++ areas simultaneously, however when the GOLIATH magnet is on, the muon beam trajectory that reaches GIF++ is deflected from its normal center. Since H4 beam line is usually overbooked, and in order for users in both areas to coexist, the precise position of the deflected muon beam in GIF++ must be known. The purpose of this study was to simulate and analyze the beam composition as well as the trajectory of muons through the interesting user zones, in order for the GIF++ users to optimally position equipment inside the facility even with the presence of the magnetic field of GOLIATH.

1.2 Muon Beam

The simulations were performed using the GEANT4-based Monte-Carlo software G4Beamline [3]. The shielding of the H4 beam line was modeled in detail (Fig. 1A) and implemented into an existing model [4]. The incident secondary beam was defined to have a nominal momentum of 150 GeV/c with Gaussian spread $\Delta p/p = 0.67\%$ (based on the typical collimator settings) and a mixed composition of 43% positively charged pions, 53% protons, and 4% positively charged kaons, which is the typical composition of the beam in H4 at this momentum [5]. The beam was simulated to impinge on collimators 9/10 in the "closed x" or "closed x & y" configuration (Fig. 1B). Each condition was simulated for 106 particles incident on the collimator.

1.3 GOLIATH

The yoke and coils of GOLIATH were modeled in detail with the appropriate materials for the yoke/pole pieces (iron), upper coil (aluminum) and lower coil (copper) [6]. The yoke and coils were positioned such that the beam was traversing at a position of 355 mm above the top edge of the bottom coil of GOLIATH, and 755 mm below the bottom edge of the top coil of GOLIATH. The most recent GOLIATH magnetic field maps to date [7] were incorporated into the simulation. The magnetic field

maps span the region, measured with x and y with respect to the beam and z with respect to the center of GOLIATH: -718.6 mm ≤ x ≤ 841.4 mm, -234.4 mm ≤ y ≤ 591.6 mm and -1762.7 mm ≤ z ≤ 1837.3 mm, in increments of 40, 59 and 50 mm respectively. The -1.5T magnetic field map was taken by setting 3600A in the top and bottom coils of GOLIATH, with an additional 1750A in the bottom coil from the DAVID power supply. The -1.0T field map was taken by setting 2400A in the top and bottom coils of GOLIATH, with an additional 1166.7A in the bottom coil from the DAVID power supply. The +1.5T and +1.0T field maps were obtained by inverting the -1.5T and -1.0T maps in the y direction.

1.4 Beam Dumps

The different zones along the beam line are separated by mobile dumps (XTDV's), which have been incorporated in the model. The interesting ones here are designated XTDV.022.520 (separating PPE-134/PPE-144), XTDV.022.610 (separating PPE-144/GIF++), and XTDV.022.628 (separating GIF++ and PPE-164), which are located as shown in Figs. 1 and 2. These dumps consist of 3.22 m of iron which can be placed on or removed from the path of the beam, thus offering flexibility of access in the downstream zones. While high-energy muons are mostly unaffected by the iron, all hadrons are absorbed by the dumps. The muon beam, produced by incidence on collimators 9/10, was studied for the four different possible combinations of opening/closing the two dumps (XTDV.022.520 & XTDV.022.610) upstream of GIF++.

1.5 Particle Scoring

Simulated data were scored at four locations inside GIF++ as described in Fig. 2. Our coordinate system defines z downstream along the beam axis, y vertically upward, and x to the left, such that the coordinate system is "right-handed." Particles were analyzed in y in the 4 meter space above the hall floor (lying -2.06 m below the beam, and 1.94 m above the beam). Cuts in x were made to display the usable beam between the walls of each location, the x positions of which are also indicated in Fig. 2. The distances are defined in meters form the T2 target.

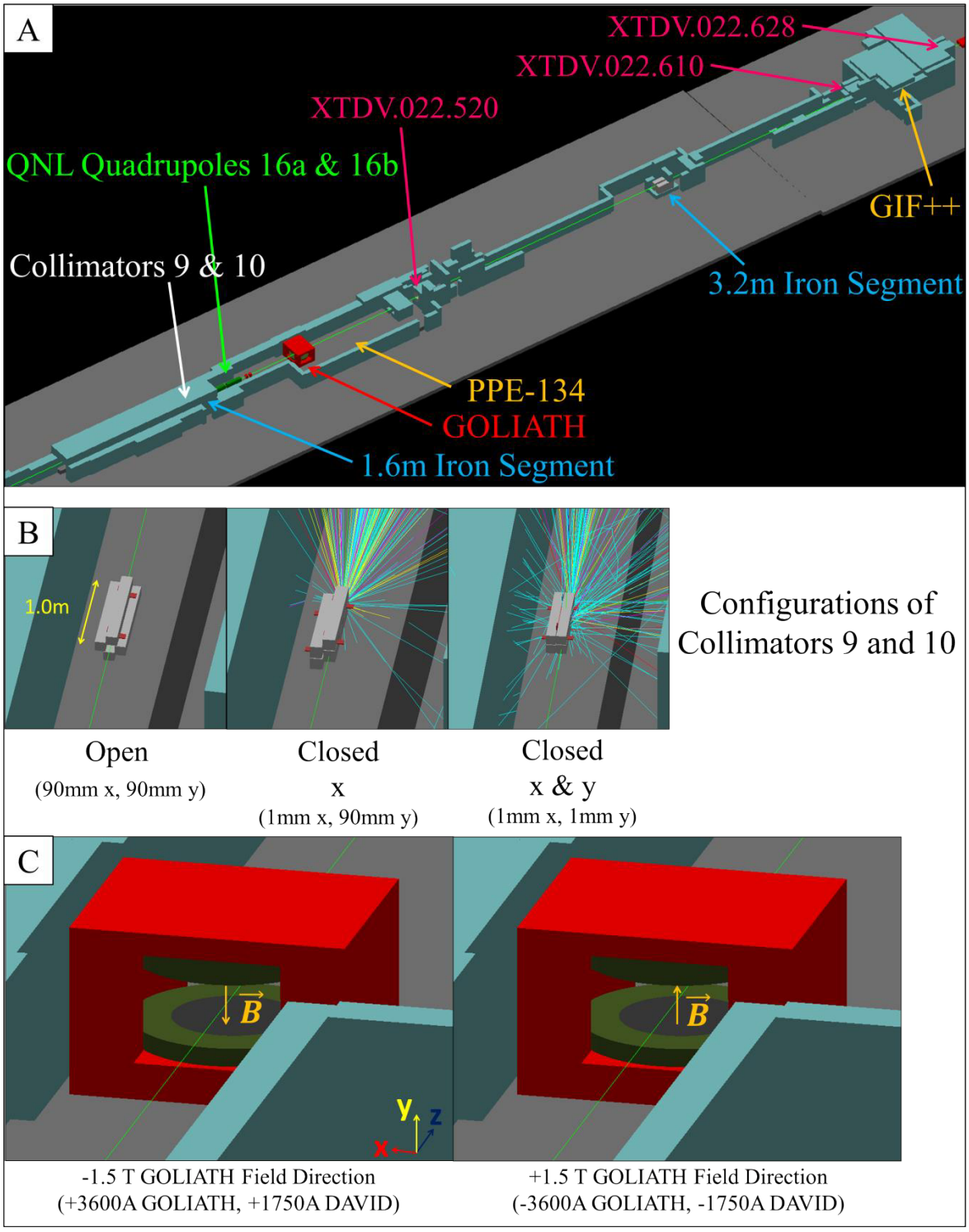

Fig. 1: (A): The layout of PPE-134 and GIF++ zones of the H4 beam line, and the G4BeamLine model details. The GOLIATH magnet is depicted in red, while the shielding blocks are in blue. (B): Possible configurations of Collimators 9 and 10. The collimators' aperture width can be set between 1 mm and 90 mm. Captions indicate the width of the aperture in x (horizontal) and y (vertical). In the closed conformations, the center of the beam is shifted to hit the center of the lower right collimator jaw (as viewed from upstream). (C): Coordinate system sign convention for the magnetic field of GOLIATH. A -1.5T field is directed vertically downward, while a +1.5T field is directed vertically upward.

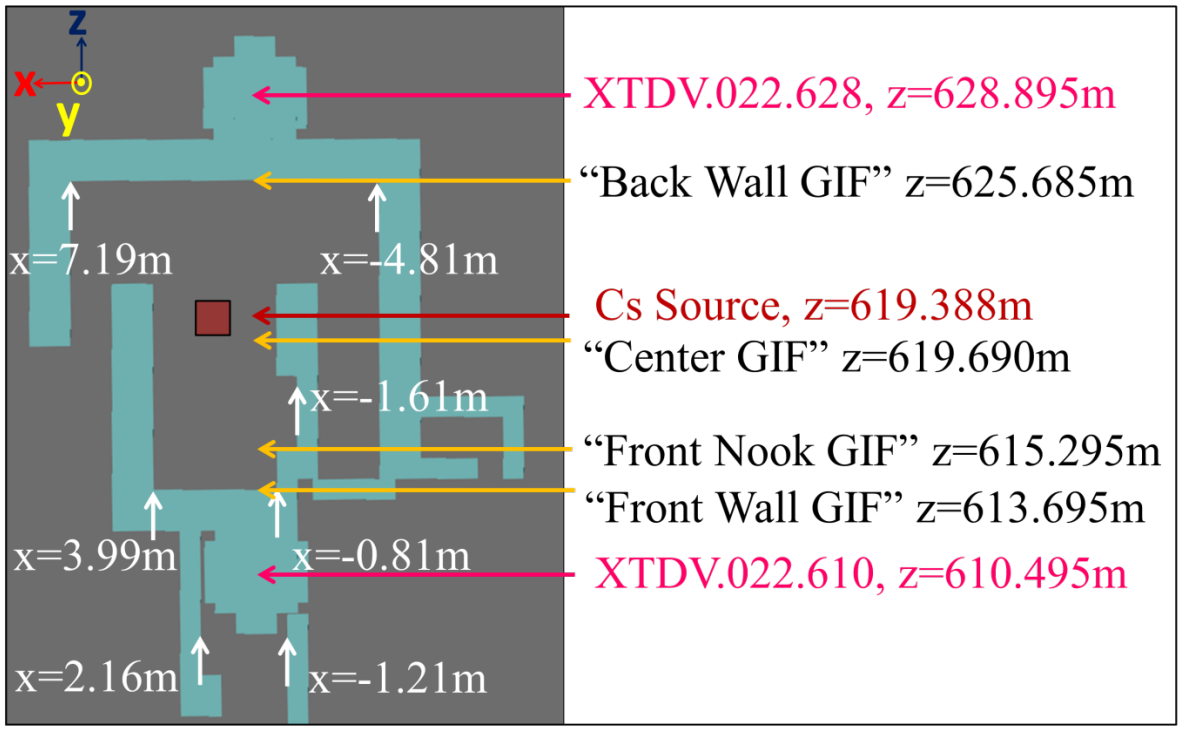

Fig. 2: z Positions of interest. The numbers correspond to distance (in m) from the T2 target of the H4 beam line up to the center of each element. Position cuts are subsequently made in x to give the available particles between the walls present at that z position, which are also indicated on the figure.

2 Results

2.1 x and y Position Plots

We plotted the x and y positions of negative (μ^-) and positive muons (μ^+) at our four z locations of interest within GIF++. Figs. 3-6 give plots for the condition where the collimator was in the "closed x" configuration, and XTDV.022.520 and XTDV.022.610 were both closed, as the strength of GOLIATH was varied. All results have been normalized to 106 particles incident on the collimator. The data analysis was done using ROOT version 5.34/34 [8].

As can be seen from Fig. 3, the horizontal position of the beam arriving at GIF++ shifts from roughly +1 m to -1 m as the GOLIATH magnet strength was varied from -1.5T to +1.5T. In the +1.0T and +1.5T cases, this shift caused the beam to traverse the wall of the GIF++ facility, thus being inaccessible to users. The y position of the beam remained centered on the nominal beam axis, as expected. Further analysis of the exact location of the center of the beam is given in section 2.2.

Concerning the beam composition, by starting with a positive hadron beam, naturally the muon beam is dominated by μ^+. For the conditions depicted, the ratio of μ^-/μ^+ ranged from 0.38% to 1.63% depending on the location and magnet strength.

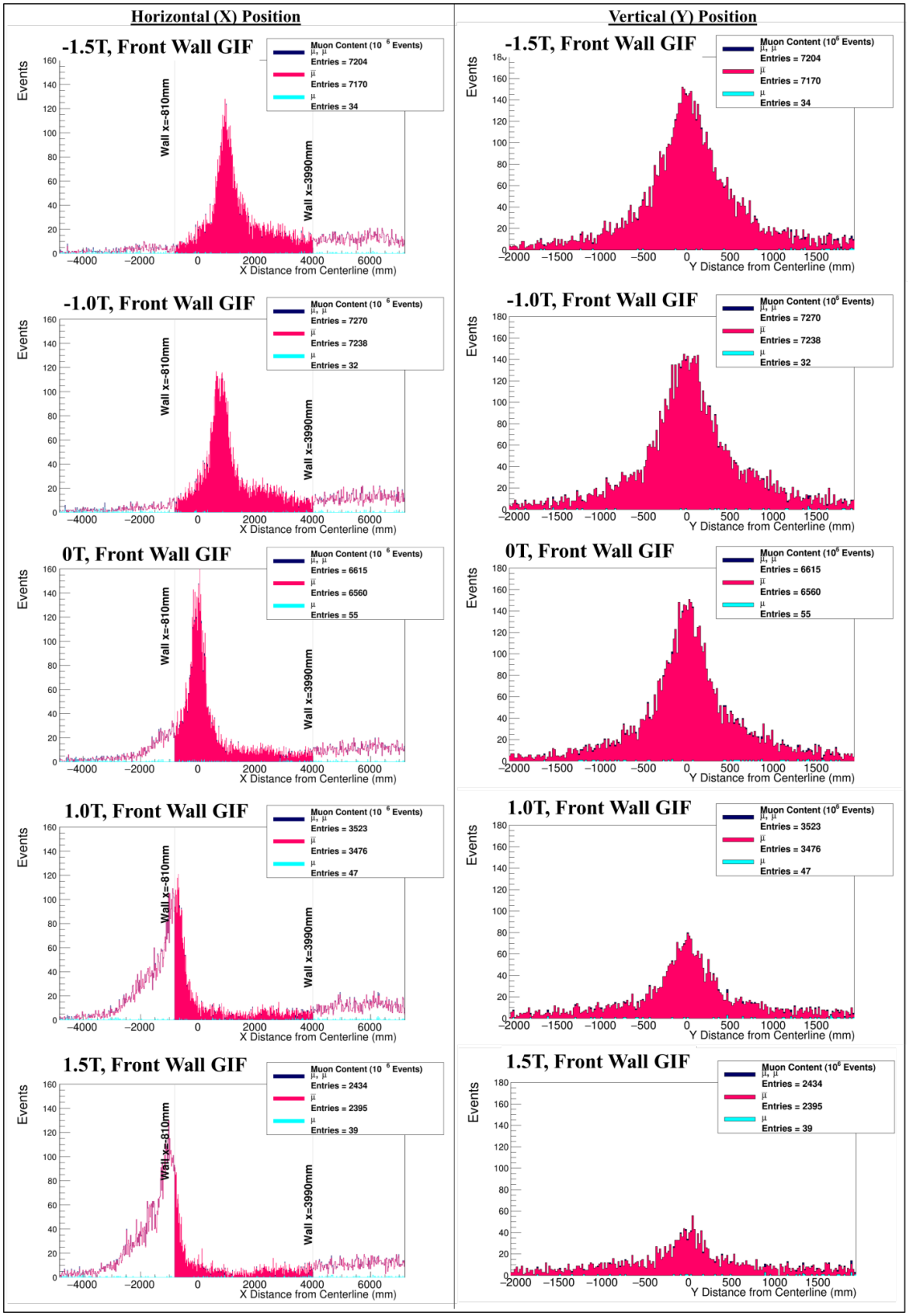

Fig. 3: Muon position plots, at position "Front GIF". μ^+ and μ^- are plotted in x and y at the "Front GIF" location (z = 613.695 m) at five different magnet strengths with the collimator in the "closed x" configuration and XTDV.022.520 and XTDV.022.610 are both closed. Only particles passing between the walls of the GIF++ facility are counted.

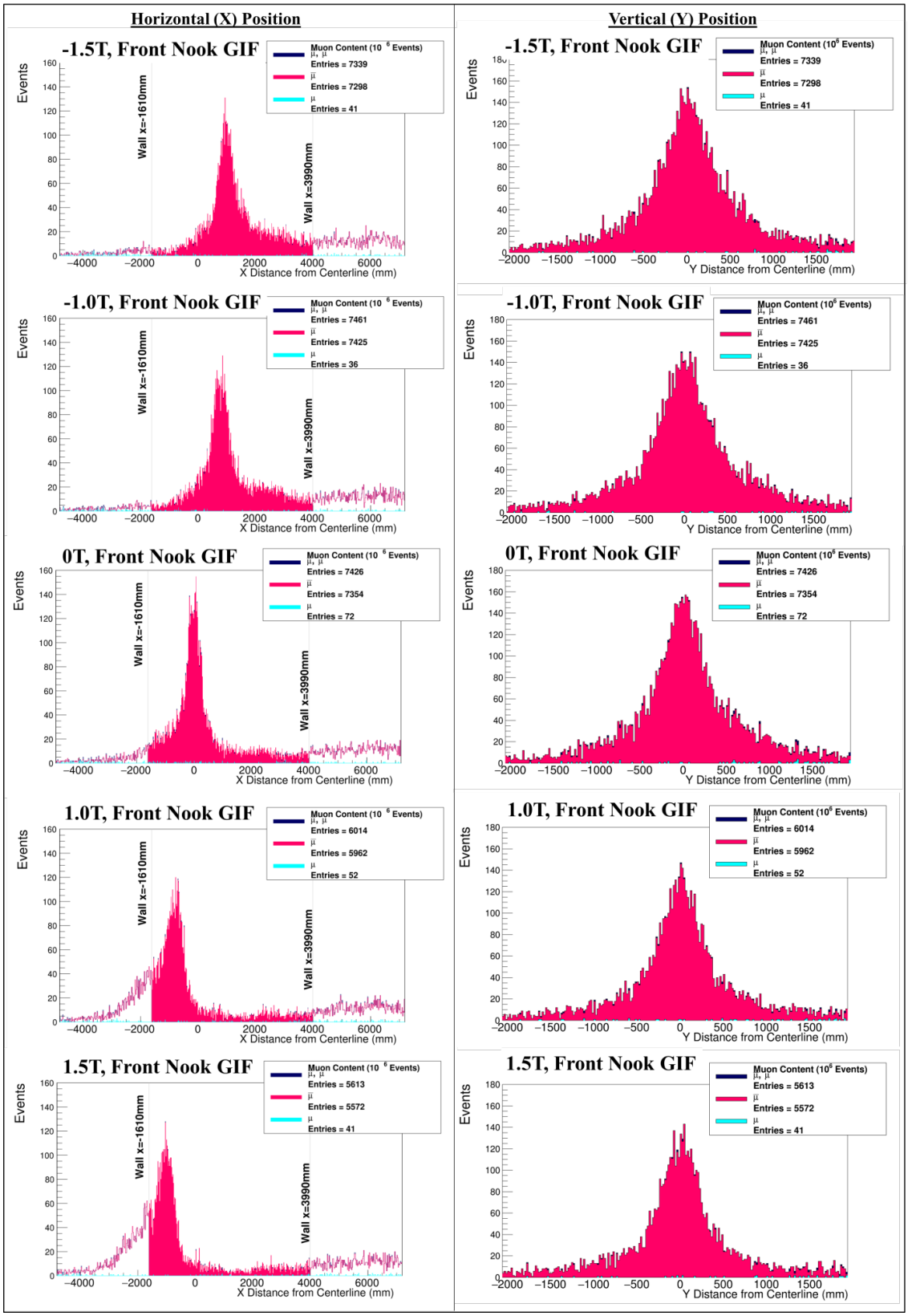

Fig. 4: Muon position plots, at position "Front Nook GIF." μ^+ and μ^- are plotted in x and y at the "Front Nook GIF" location (z = 615.295 m) at five different magnet strengths with the collimator in the "closed x" configuration and XTDV.022.520 and XTDV.022.610 are both closed. Only particles passing between the walls of the GIF++ facility are counted.

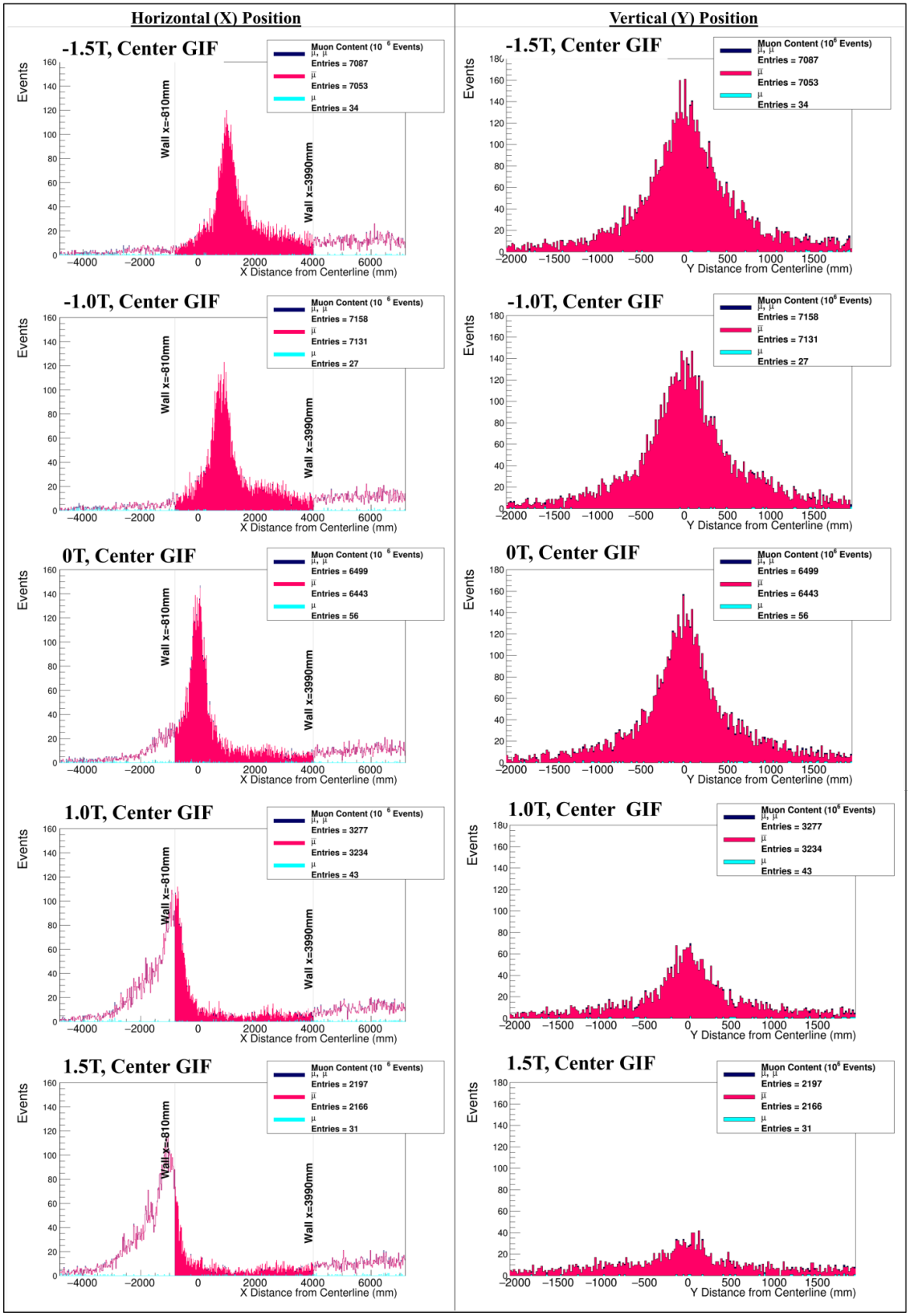

Fig. 5: Muon position plots, at position "Center GIF." μ^+ and μ^- are plotted in x and y at the "Center GIF" location (z = 619.690 m) at five different magnet strengths with the collimator in the "closed x" configuration and XTDV.022.520 and XTDV.022.610 are both closed. Only particles passing between the walls of the GIF++ facility are counted.

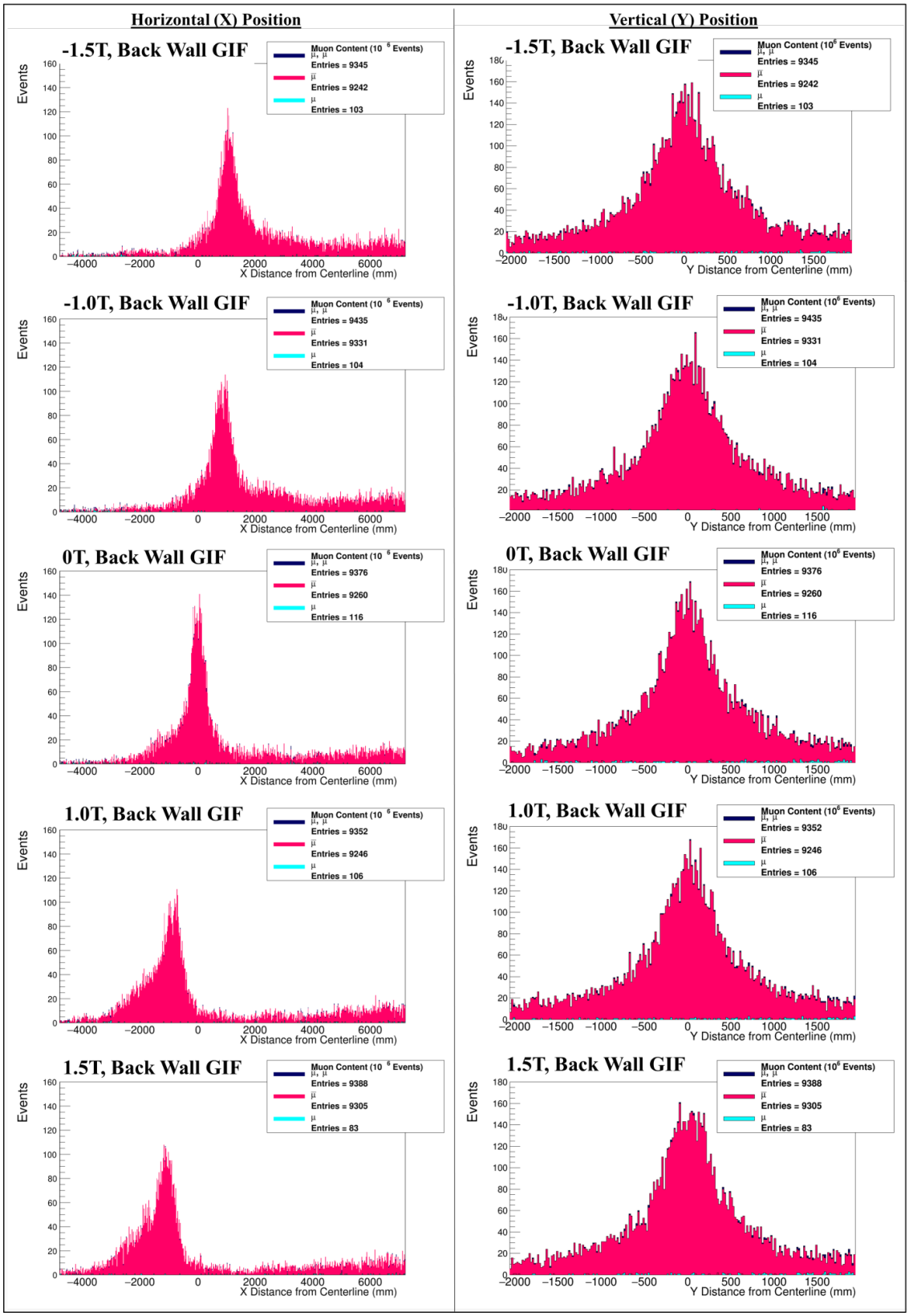

Fig. 6: Muon position plots, at position "Back Wall GIF." μ^+ and μ^- are plotted in x and y at the "Back Wall GIF" location (z = 625.685 m) at five different magnet strengths with the collimator in the "closed x" configuration and XTDV.022.520 and XTDV.022.610 are both closed. Only particles passing between the walls of the GIF++ facility are counted.

2.2 x vs y Position Plots and Muon Momentum Distribution

In the next plots, the x vs y position and overall momentum distribution of μ^- and μ^+ at four z locations of interest within GIF++ are shown. Figs. 7-10 depict the muon population for the condition where the collimator was in the "closed x" configuration and both dumps were closed. Again, five different magnet strengths were tested. All results have been normalized for 10^6 particles incident on the collimator.

The GIF++ facility is horizontally asymmetric; the "right" (-x) wall of the facility is closer to the nominal position of the beam than the "left" (+x) wall. Due to this asymmetrical positioning of the facility, the spatial region where usable muons are analyzed is also asymmetric. For example, at the "Front Wall GIF" position, muons are analyzed between x = -.81m to x = 3.99 m, as shown in Fig. 2. Therefore, if the average position of these muons is taken, it will be artificially weighted to the right.

It was deemed more useful to instead analyze the position of the most intense region of the muon beam. This "peak muon distribution" region was defined to include only histogram bins (50 mm x 50 mm) containing at least 20 $\mu^- + \mu^+$ counts (per 10^6 particles incident on the collimator) with momentum at least 20 GeV/c. This corresponds to a muon density of at least 0.008 muons per mm^2 per 10^6 particles. Bins meeting the criteria of the peak muon distribution are outlined in black in Figs. 7-10. Note that the standard deviation of muon position in the peak muon distribution, given in the legend of each figure, was based solely on bins in the peak muon distribution. The actual beam is broader than these standard deviations suggest.

These plots clearly show dependence of the x position of the peak muon beam on the strength of GOLIATH. At the "Back Wall GIF" location, the x position of the peak muon beam shifted from 1088 mm at -1.5T, to 815 mm at -1.0T, -9 mm at 0T, -797 mm at +1.0T and -1160 mm at +1.5T.

The momentum distribution plots show a broad range of μ^+ momenta ranging from 0 to approximately 135 GeV/c. Further analysis of the momentum of muons in the peak muon distribution is given in section 2.3.

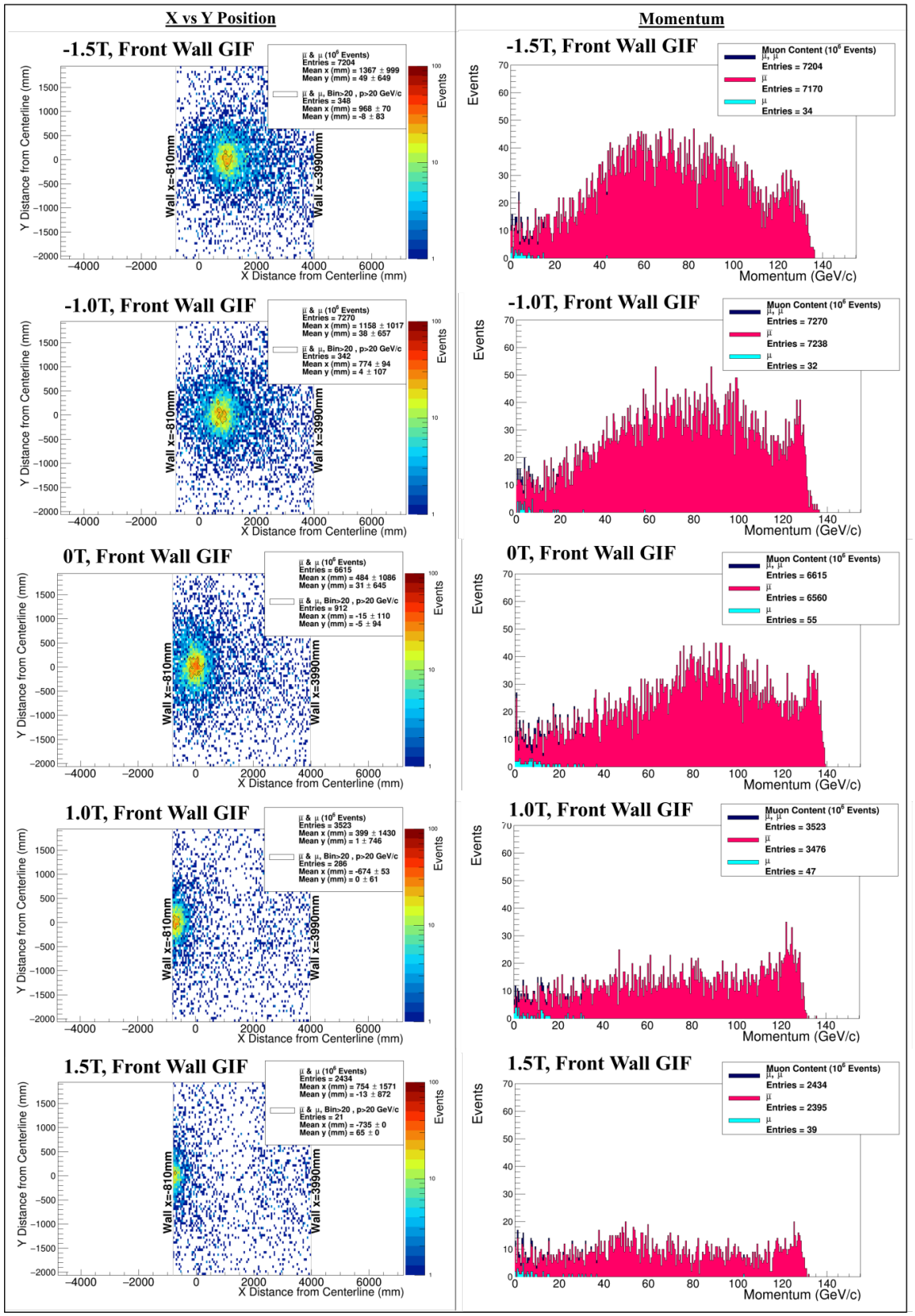

Fig. 7: Muon x-y position and momentum distribution at position "Front GIF." μ^+ and μ^- are plotted for x vs y and for overall momentum at the "Front GIF" location (z = 613.695 m) at five different magnet strengths with the collimator in the "closed x" configuration and XTDV.022.520 and XTDV.022.610 both closed. Only particles passing between the walls of the GIF++ facility are counted.

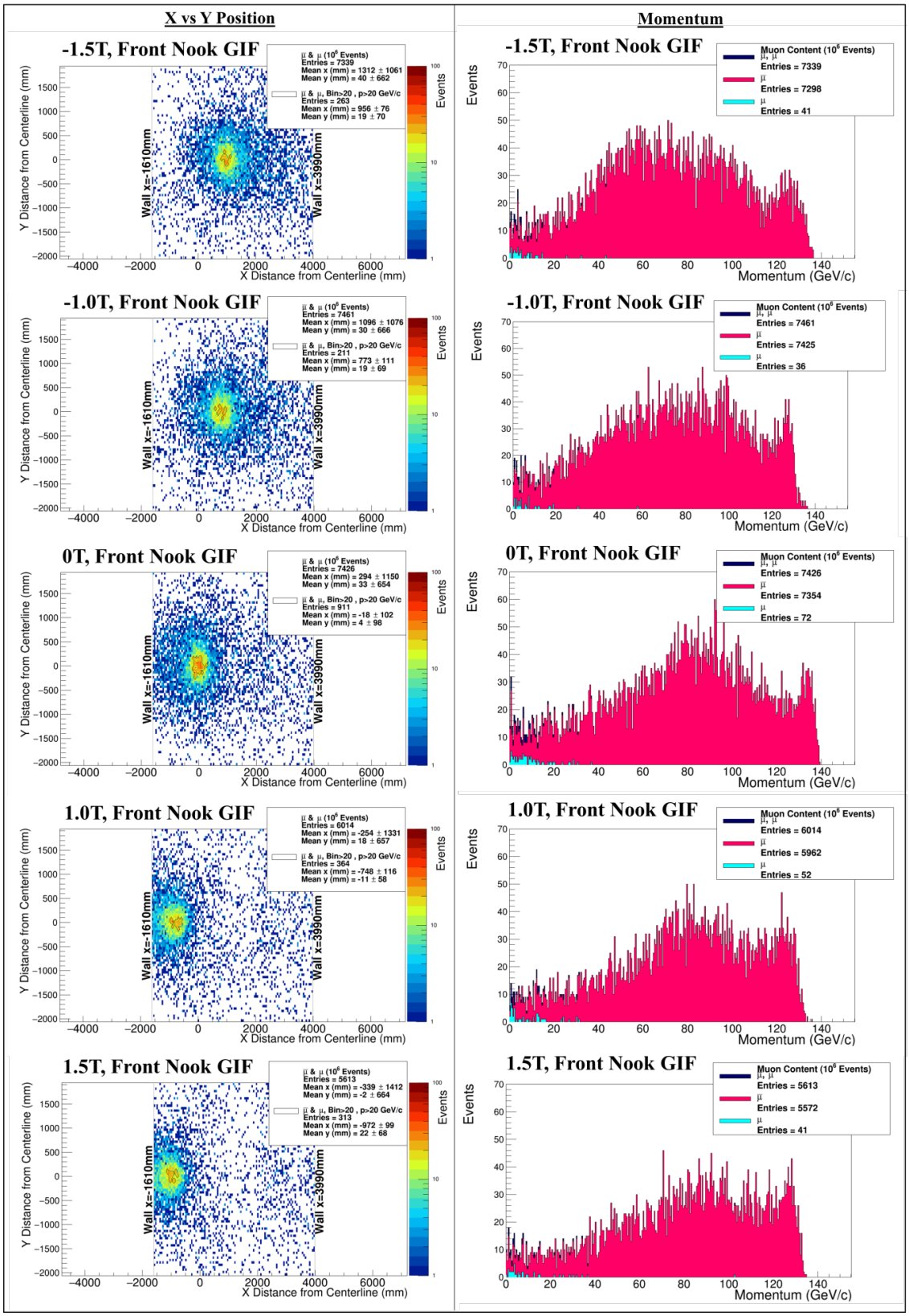

Fig. 8: Muon x-y position and momentum distribution at position "Front Nook GIF." μ^+ and μ^- are plotted for x vs y and for overall momentum at the "Front Nook GIF" location (z = 615.295 m) at five different magnet strengths with the collimator in the "closed x" configuration and XTDV.022.520 and XTDV.022.610 both closed. Only particles passing between the walls of the GIF++ facility are counted.

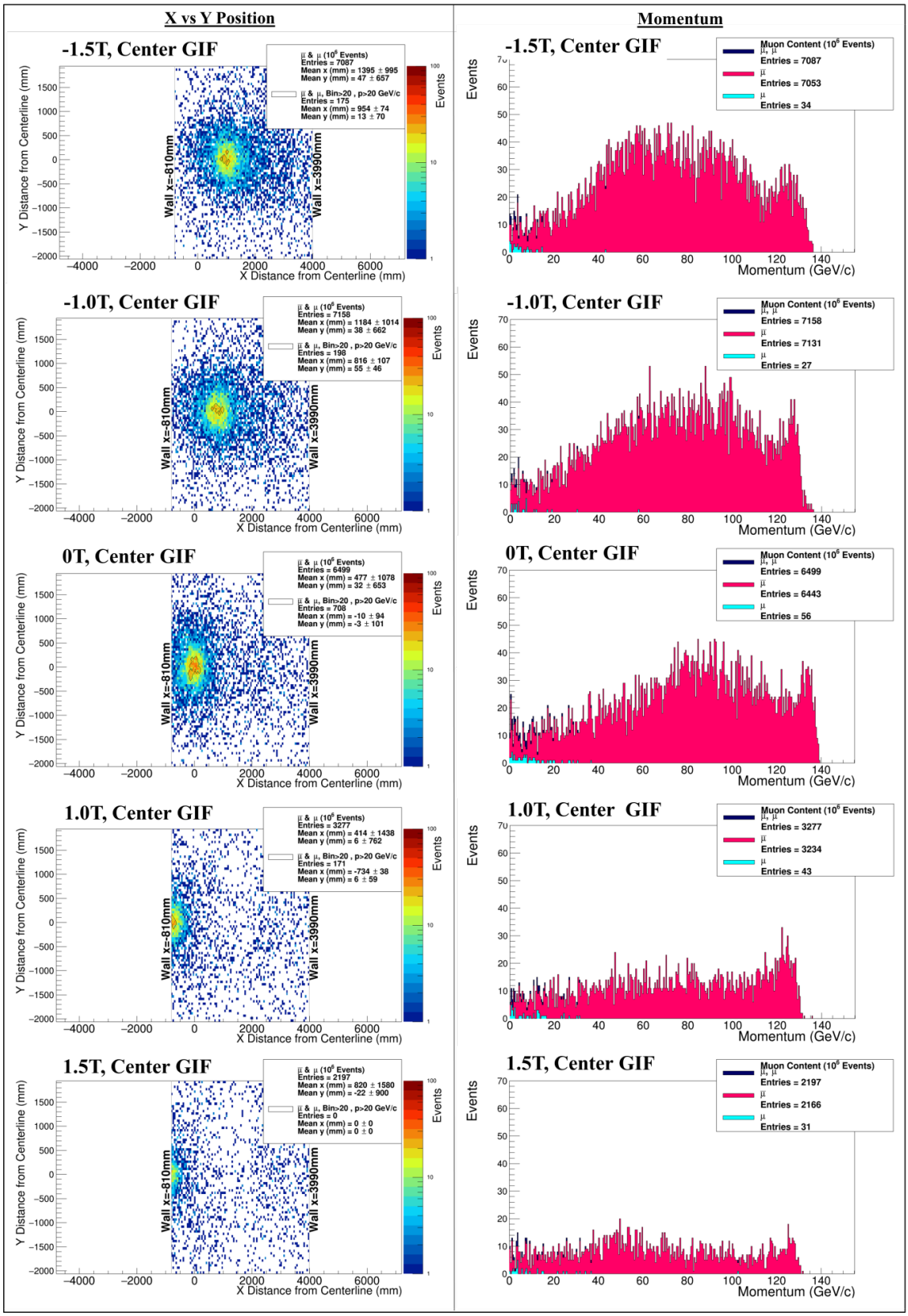

Fig. 9: Muon x-y position and momentum distribution at position "Center GIF." μ^+ and μ^- are plotted for x vs y and for overall momentum at the "Center GIF" location (z = 619.690 m) at five different magnet strengths with the collimator in the "closed x" configuration and XTDV.022.520 and XTDV.022.610 both closed. Only particles passing between the walls of the GIF++ facility are counted.

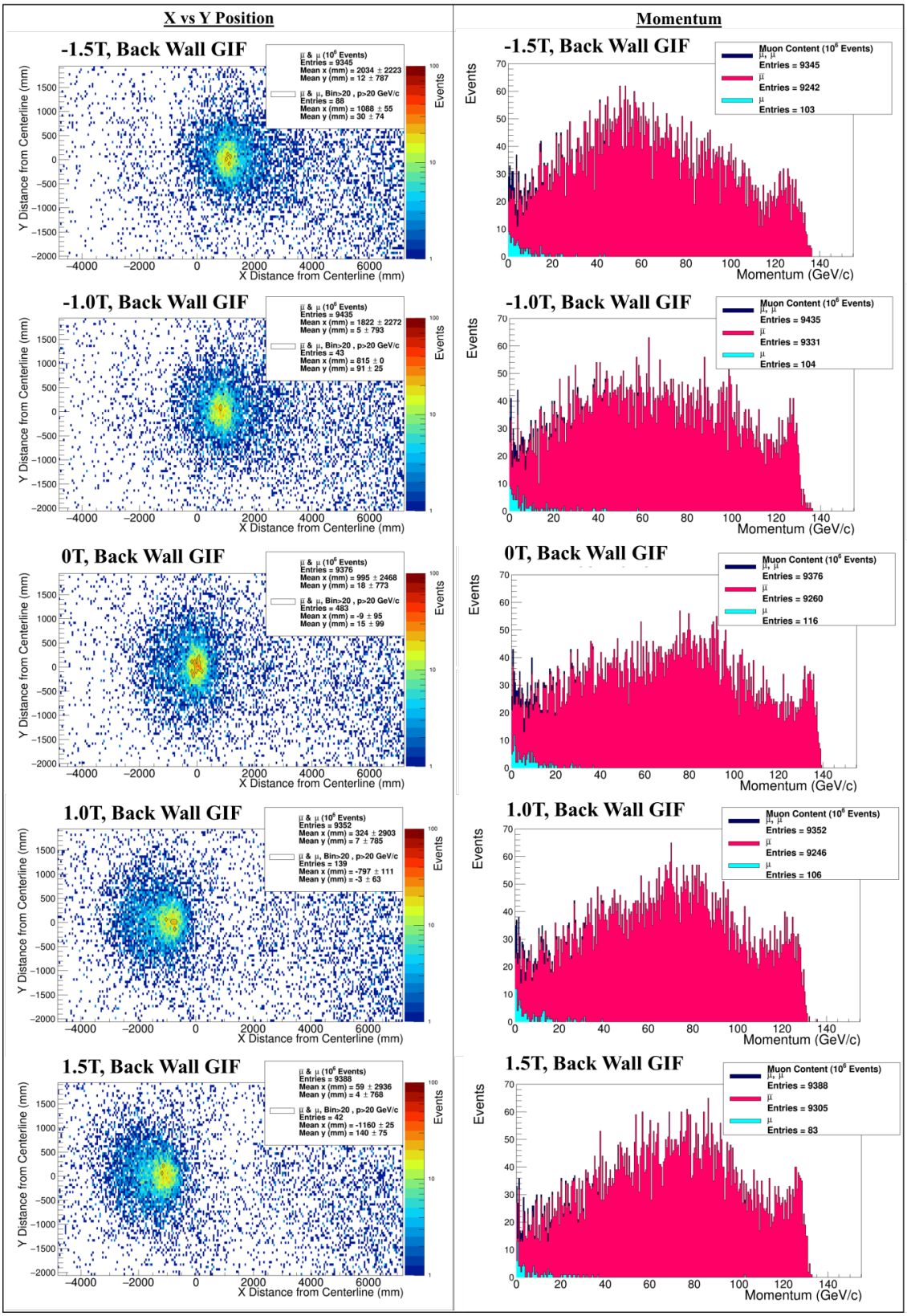

Fig. 10: Muon x-y position and momentum distribution at position "Back Wall GIF." μ^+ and μ^- are plotted for x vs y and for overall momentum at the "Back Wall GIF" location (z = 625.685 m) at five different magnet strengths with the collimator in the "closed x" configuration and XTDV.022.520 and XTDV.022.610 both closed. Only particles passing between the walls of the GIF++ facility are counted.

2.3 x vs Momentum and y vs Momentum Distributions

The magnetic field of GOLIATH causes dispersion (momentum dependent angle and position) in the horizontal plane which is quite prominent at GIF++ due to the large distance between the dipole and the facility. Figs. 11-14 show the momentum distribution versus x and y positions of μ^- and μ^+ at the four selected z locations of interest within the GIF++ facility. In all these simulations, the collimator was in the "closed x" configuration, and XTDV.022.520 and XTDV.022.610 were both closed, at five different magnet strengths. Simulations were run for 10^6 particles incident on the collimator.

As with Figs. 7-10, the asymmetrical design of the GIF++ facility causes an artificial offset in the calculated x position of the overall muon beam, necessitating the analysis of a peak muon distribution instead of analysis of the overall muon distribution. This peak muon distribution region was defined to include only histogram bins (50 mm x 5 GeV/c) containing at least 20 $\mu^- + \mu^+$ counts (per 10^6 particles incident on the collimator) with momentum at least 20 GeV/c. Bins meeting the criteria of this peak muon distribution are outlined in black in Figs. 11-14. This peak distribution was used to calculate the mean position and momentum of the peak beam, as shown in the legends of Figs. 11-14.

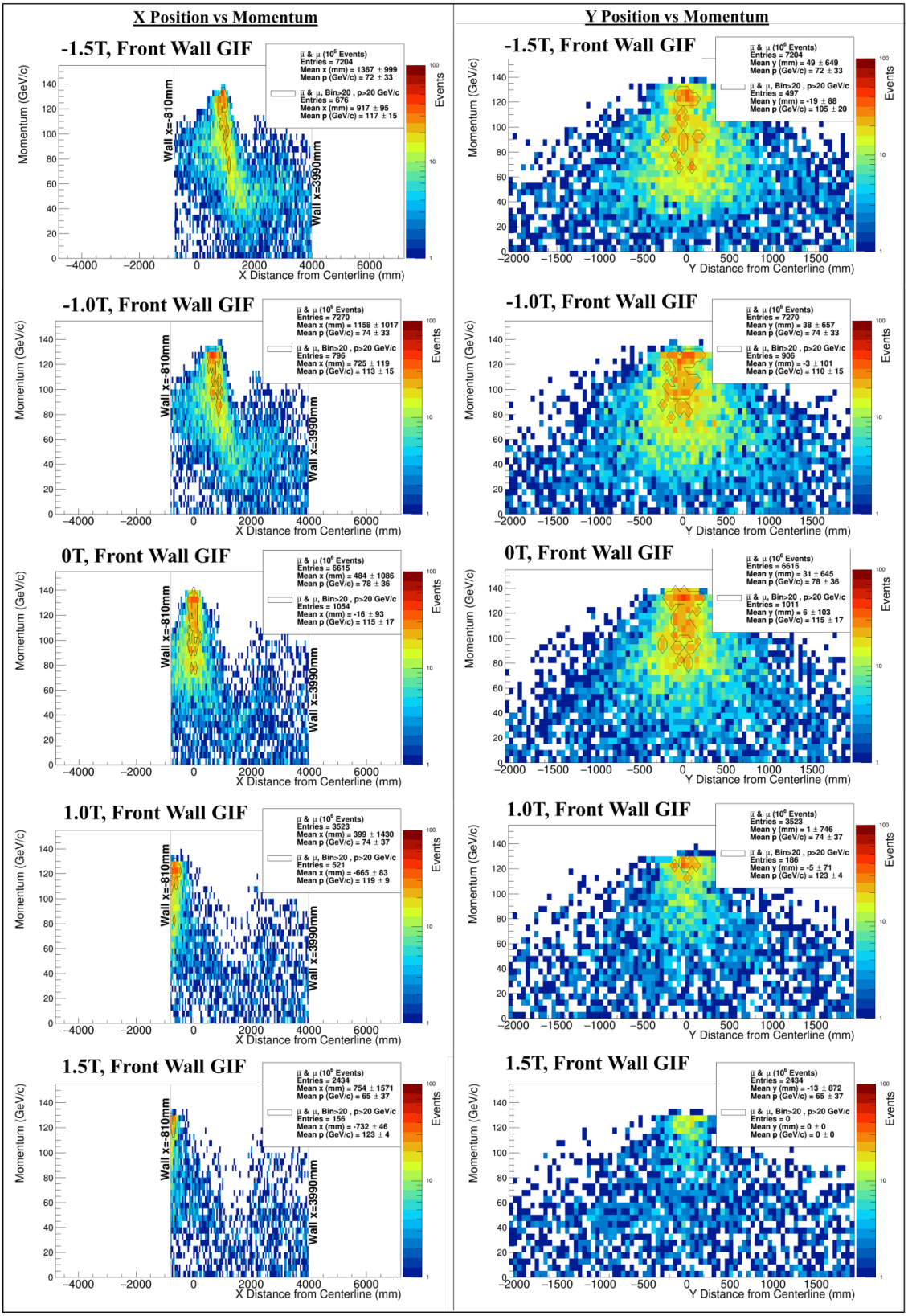

Fig. 11: Momentum distribution of muons vs x and y, at position "Front GIF μ^+ and μ^- are plotted for momentum vs x and y at the "Front GIF" location (z = 613.695 m) at five different magnet strengths with the collimator in the "closed x" configuration and XTDV.022.520 and XTDV.022.610 are both closed. Only particles passing between the walls of the GIF++ facility are counted.

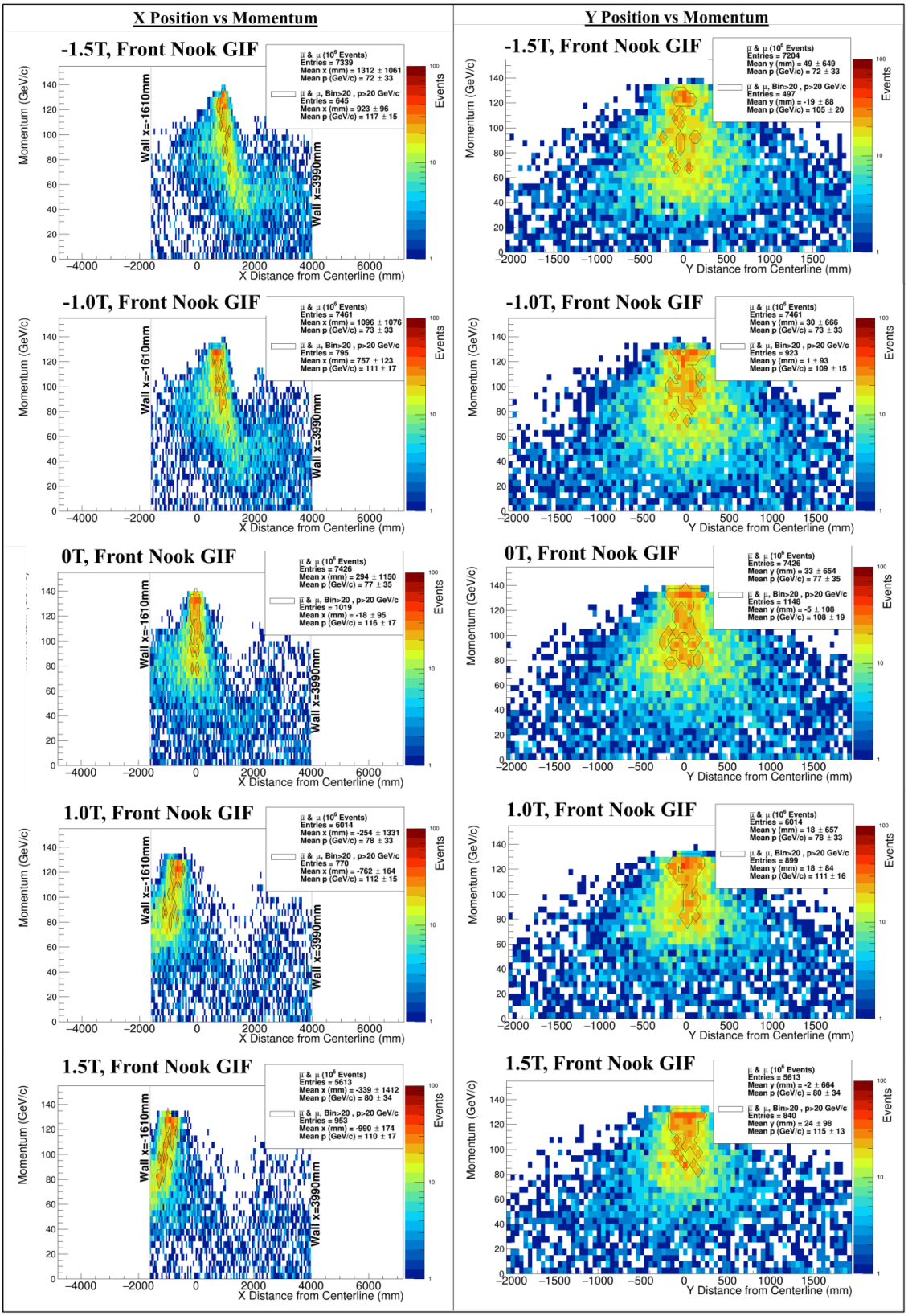

Fig. 12: Momentum distribution of muons vs x and y, at position "Front Nook GIF." μ^+ and μ^- are plotted for momentum vs x and y at the "Front Nook GIF" location (z = 615.295 m) at five different magnet strengths with the collimator in the "closed x" configuration and XTDV.022.520 and XTDV.022.610 are both closed. Only particles passing between the walls of the GIF++ facility are counted.

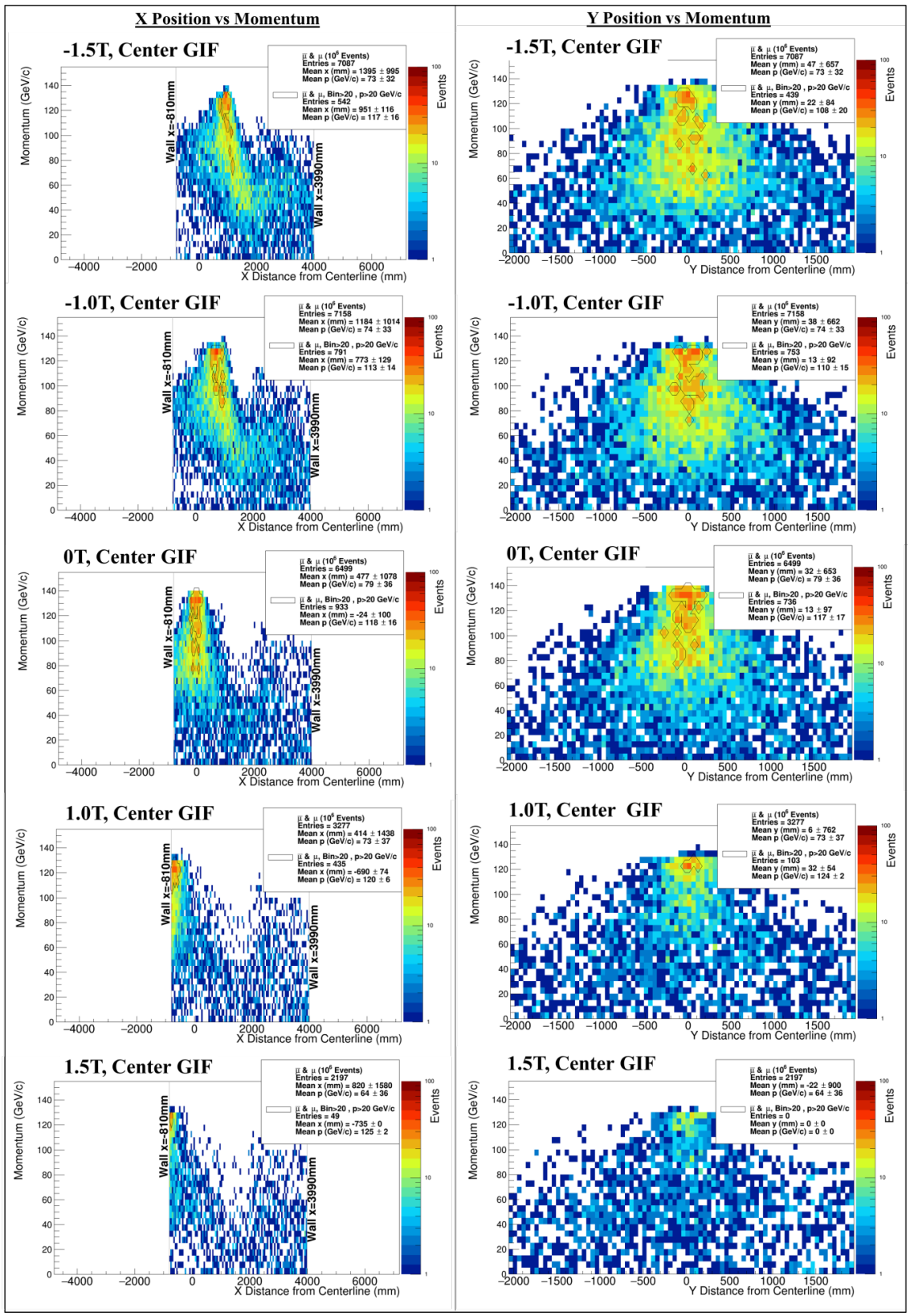

Fig. 13: Momentum distribution of muons vs x and y, at position "Center GIF." μ^+ and μ^- are plotted for momentum vs x and y at the "Center GIF" location (z = 619.690 m) at five different magnet strengths with the collimator in the "closed x" configuration and XTDV.022.520 and XTDV.022.610 are both closed. Only particles passing between the walls of the GIF++ facility are counted.

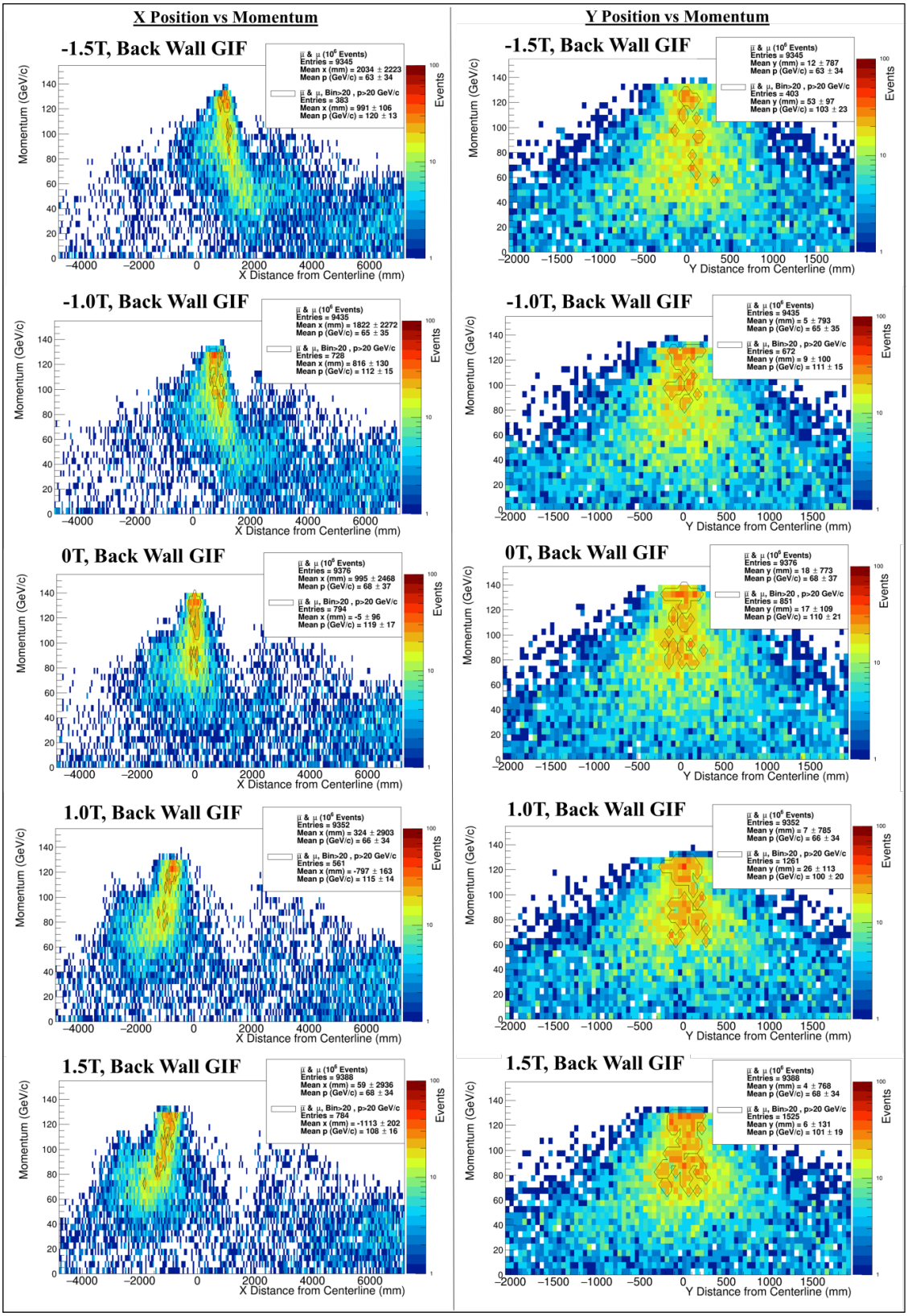

Fig. 14: Momentum distribution of muons vs x and y, at position "Back Wall GIF." μ^+ and μ^- are plotted for momentum vs x and y at the "Back Wall GIF" location (z = 625.685 m) at five different magnet strengths with the collimator in the "closed x" configuration and XTDV.022.520 and XTDV.022.610 are both closed. Only particles passing between the walls of the GIF++ facility are counted.

2.4 Different beam Conditions

We tested 40 different beam line configurations by testing different combinations of setting the collimator to the "closed x" or "closed x & y" configuration, varying the strength of GOLIATH, and opening/closing XTDV.022.520 and XTDV.022.610. We then studied the rate of positive pion (π^+) and negative pion (π^-) contamination, the rate of muons in the peak distribution and overall usable beam, and the mean x and y positions of the peak $\mu^+ + \mu^-$ distribution. Simulations were run for 10^6 particles incident on the collimator. Selected configurations are shown in Figs. 15-17, and more data are available in electronic form by request.

In general, pion contamination was found to be less than 50 $\pi^+ + \pi^-$ counts, with a pion to muon ratio ($(\pi^+ + \pi^-)/(\mu^+ + \mu^-)$) of 1% or less, for all cases except beams where the field of GOLIATH was set to zero and both XTDV dumps were open. In the latter case, the pion contamination rate increased up to a maximum 3368 $\pi^+ + \pi^-$ counts with a pion to muon ratio of 46.8% at the "Front Wall GIF" location (Fig. 15). Even if this pion rate seems counter-intuitive, it can be explained by the fact that the pion beam entering the facility is towards the Saleve (-x) side, resulting in a big part of the muon beam being lost outside the walls of GIF++. The total number of pions scored at the "Center GIF" location amount to 0.7% of the initial pion population impinging on the collimator, well in agreement with the ~5 interaction lengths corresponding to the collimator material. The situations improves by closing one or more of the XTDV dumps.

Closing the XTDV dumps made a large difference in the pion contamination when GOLIATH was off, however, this effect was less pronounced in the cases where GOLIATH was on. This can be explained by the fact that, when the magnet is on, the beam passes through the 3.2 m iron segment shown in Fig. 1A, and described in ref. [9].

Usable $\mu^+ + \mu^-$ rate generally varied only with magnet strength (Fig. 16), due to muons lost while traveling inside the walls of GIF++. At the "Back Wall GIF" location, the overall usable muon rate did not change much for any of the configurations tested, with a mean rate of ~10^4 $\mu^+ + \mu^-$ counts (per 10^6 incident hadrons on the collimator) across these conditions. However, the proportion of these muons within the peak distribution showed a slight increase when XTDV.022.520, was open, due to the multiple scattering caused by the 3.2 meters of iron of the XTDV. Closing XTDV.022.520 and opening XTDV.022.610, by contrast, resulted in a proportion of muons in the peak distribution which resembled the configuration where both dumps were closed.

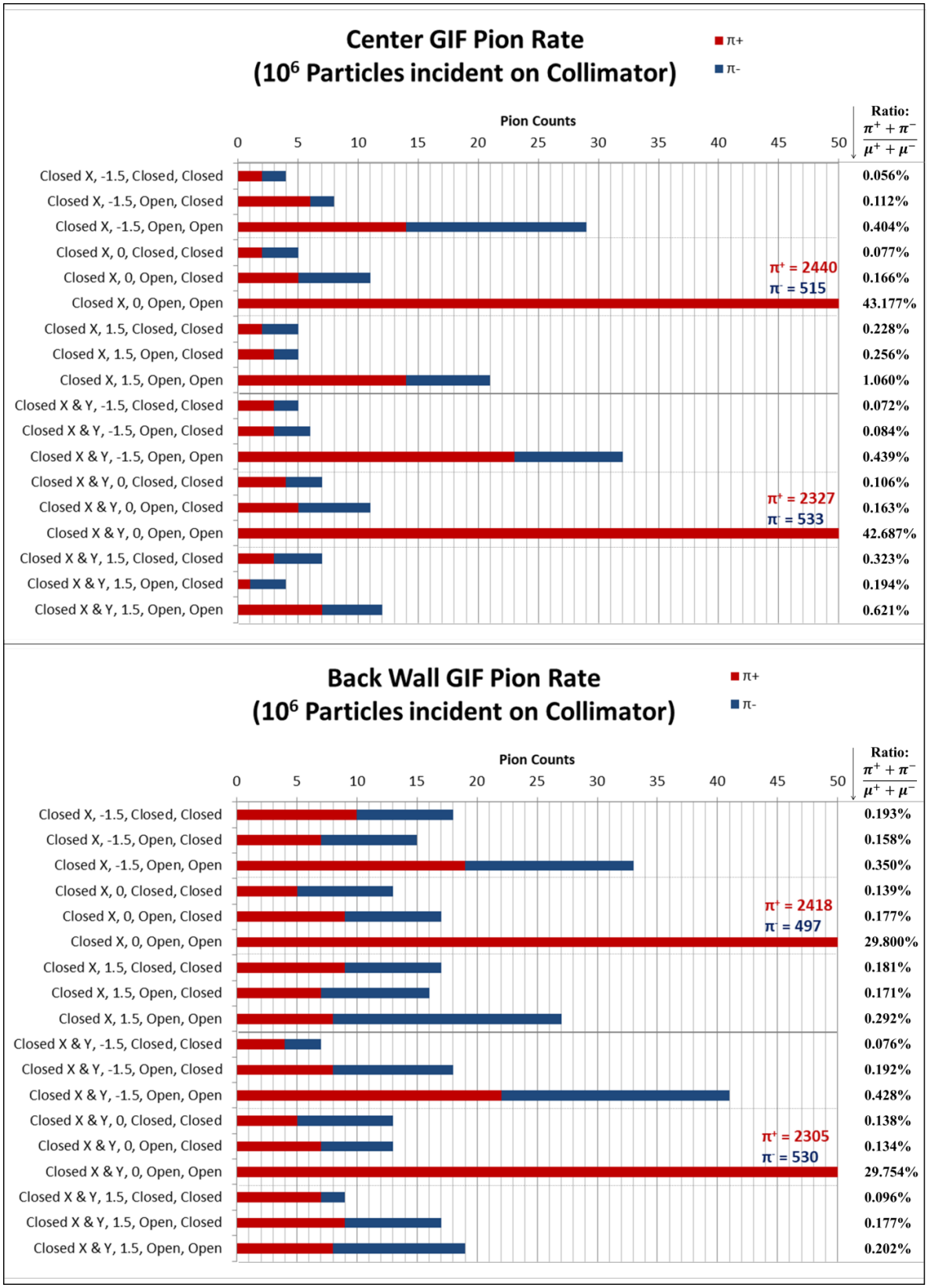

Fig. 15: Pion contamination plots. π^+ (red portion of each bar) and π^- (blue portion of each bar) counts for different beam line configurations. The first item listed is the collimator configuration, second is the strength of GOLIATH, third is the open/closed state of XTDV.022.520 and fourth is the open/closed state of XTDV.022.610. The right column describes the pion to muon ratios for each condition, converted to percentages.

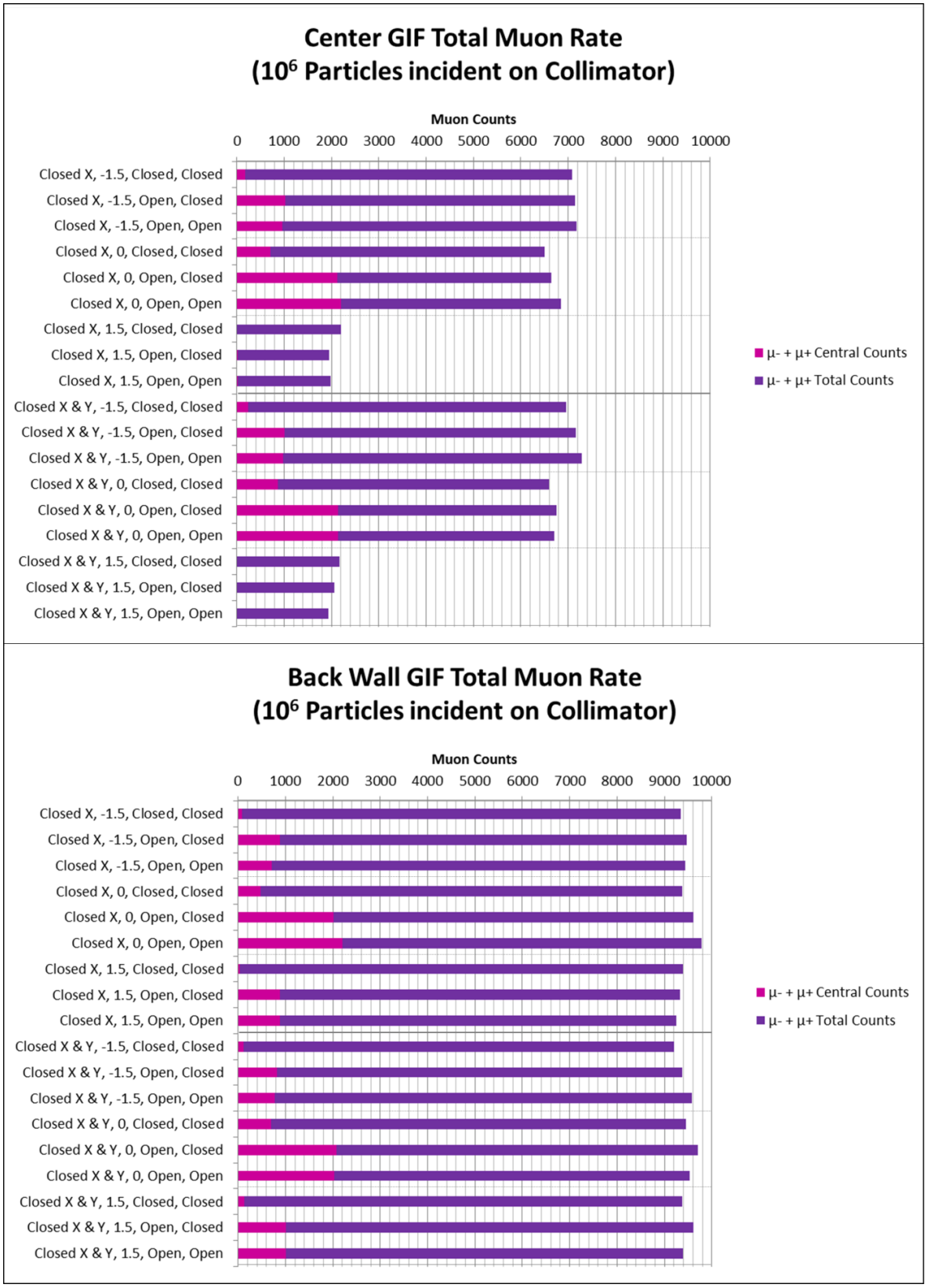

Fig. 16: Muon rate for the several different combinations of elements affecting the muon composition. $\mu^+ + \mu^-$ counts in the peak beam distribution in x and y (light purple) versus the overall usable muon rate (full length of bar), for different beam line configurations. The first item listed is the collimator configuration, second is the strength of GOLIATH, third is the open/closed state of XTDV.022.520 and fourth is the open/closed state of XTDV.022.610.

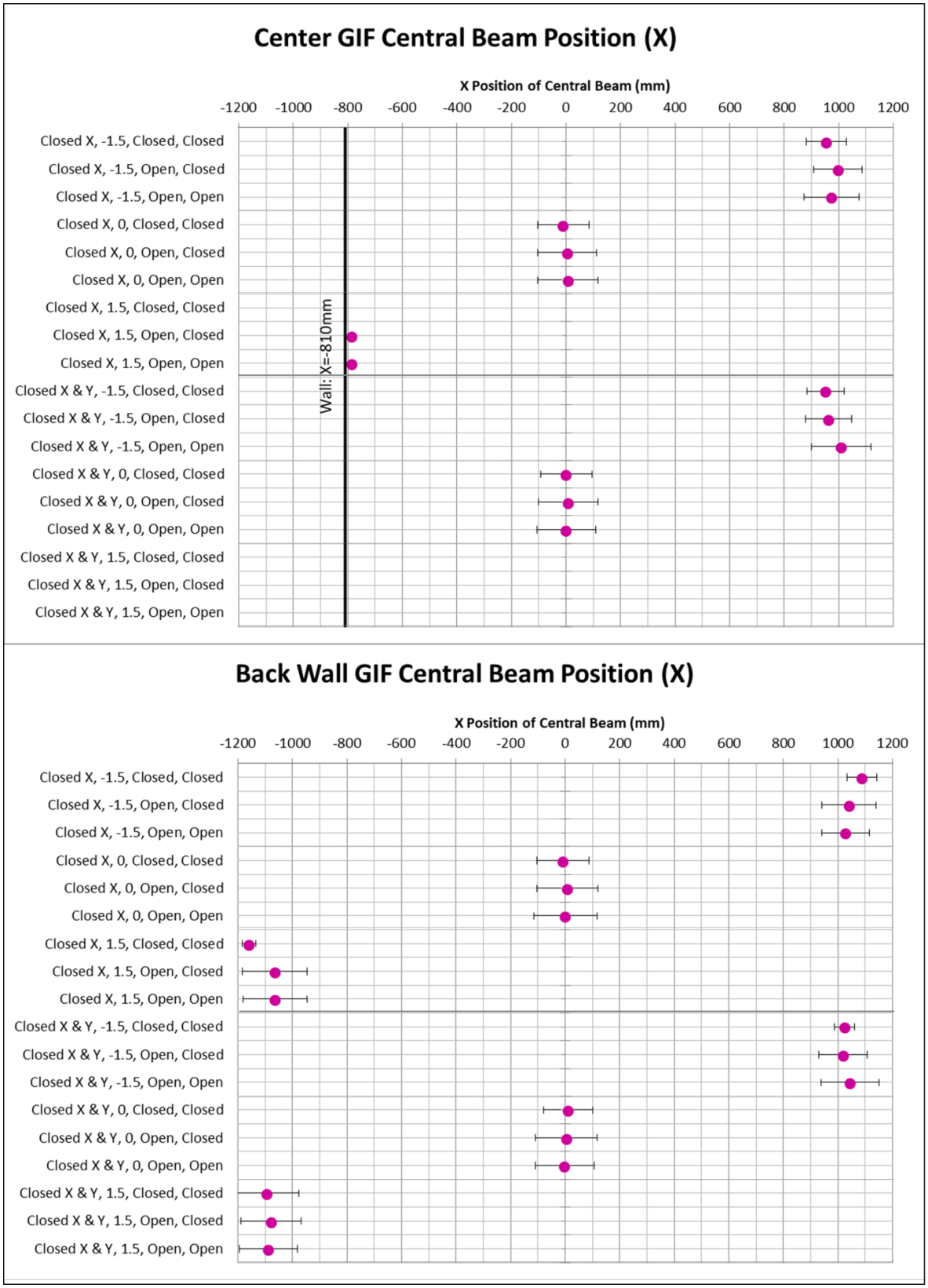

Fig. 17: Mean x position of the $\mu^+ + \mu^-$ peak beam distribution for different beam line configurations. The first item listed is the collimator configuration, second is the strength of GOLIATH, third is the open/closed state of XTDV.022.520 and fourth is the open/closed state of XTDV.022.610. Rows missing data had no bins fitting the peak beam criteria (bin > 20 counts, p > 20 GeV/c).

3 Summary and Discussion

3.1 Optimal positioning of equipment inside GIF++

The muon beam reaching GIF++ has its x position shifted based on the strength and polarity of the magnetic field of GOLIATH. For the +1.5T and +1.0T strengths of GOLIATH, this beam will pass largely through the wall of GIF++. It is therefore preferable to use the negative polarity of GOLIATH when possible, which corresponds to positive currents in the power supplies of GOLIATH and DAVID. However, when the positive polarity of GOLIATH is required, there are still smaller regions within GIF++ where equipment may be placed in order to be irradiated by muons. The gamma ray source can be moved from 0.65 m to 2.15 m in x [10], and adjusting its horizontal position can additionally increase the size of regions receiving both muon and gamma ray flux.

At the -1.5T setting, equipment may be placed either upstream or downstream of the gamma ray source, along the full length of GIF++ as shown in Fig.19A. Positioning the gamma ray source at x = 1.0 m will maximize the size of these regions. At the +1.5T setting, equipment may be placed near the back wall of GIF++, or in the nook of the right wall as shown in Fig. 19B. These areas are largest when the gamma ray source is in its closest position to the beam, 0.65 m from the nominal beam center. At either magnet setting, equipment should be placed at the nominal beam position in y.

In order to further reduce pion contamination, it is advisable to keep XTDV.022.520 and XTDV.022.610 closed, especially when GOLIATH is off. If high muon rate in the peak beam is prioritized over pion contamination, opening the upstream dump, XTDV.022.520, will slightly increase the muon rate in the peak position.

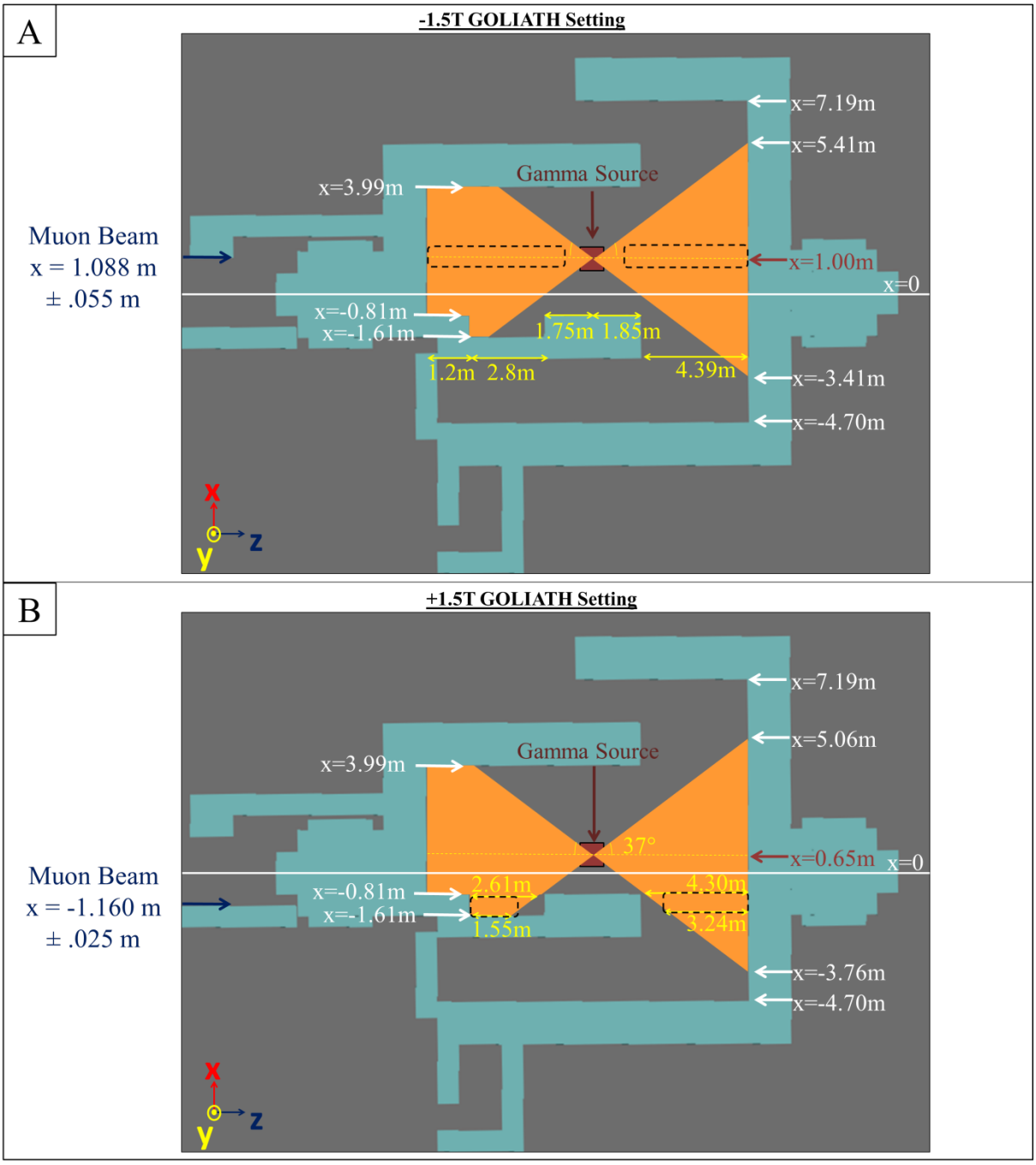

Fig. 18: Equipment placement regions to optimally receive simultaneous muon and gamma photon flux. Geometrical analysis of the gamma ray source, using the gamma source collimator half-angle of 37° is shown. The gamma ray source is analyzed in its 1.0 m and 0.65 m positions in order to achieve maximum overlap with the muon beam at the -1.5T and +1.5T GOLIATH field strengths respectively. Muon beam positions describe the mean x position of the peak muon beam at the "Back Wall GIF" location with the collimator in the "closed x" configuration and XTDV.022.520 and XTDV.022.610 both closed.

4 Acknowledgements

The authors would like to thank Marcel Rosenthal, who provided great support with G4Beamline and contributed to the GOLIATH field map utilized in this simulation. The authors would like to thank Sylvain Girod and Vincent Clerc for their guidance in perfecting the geometry of the H4 beam line. The GOLIATH field mapping was also performed with the valuable help of Yiota Chatzidaki, the EP/DT magnet group (Felix Bergsma & Pierre-Ange Giudici), Henric Wilkens and the kind support of RD51 Collaboration (Eraldo Oliveri & Yorgos Tsipolitis). The authors would like to thank also Lau Gatignon for discussions on the manuscript.

5 References

[1] G. Brianti, “SPS North Experimental Area – General Layout”, CERN/LAB II/EA/Note 73-4, (1973).

[2] "Introduction to the use of the H4 beam." CERN/EN/SBA - http://sba.web.cern.ch/sba/BeamsAndAreas/H4/H4_presentation.html

[3] T. J. Roberts, K. Beard, D. Huang, S. Ahmed, D. M. Kaplan, and L. Spentzouris, “G4BeamLine particle tracking in matter dominated beam lines”, WEPP120, Proceedings of EPAC08, Genoa, Italy.

[4] N. Charitonidis, et al., “Beam Performance and instrumentation studies for ProtoDUNE-DP experiment of CENF”, CERN-ACC-NOTE-2016-0052. (2016).

[5] H.W. Atherton, *et al.*, “Precise Measurements of Particle Production by 400 GeV/c Protons on Beryllium Targets”, CERN 80-07 (1980).

[6] W. Flegel, “GOLIATH Magnet” CERN/EP (1998).

[7] M. Rosenthal *et al.* “Magnetic Field Measurements of the GOLIATH Magnet in EHN1.” CERN-ACC-NOTE-2018-0028. (2018).

[8] R. Brun and F. Rademakers, “ROOT - An Object Oriented Data Analysis Framework”, Proceedings AIHENP'96 Workshop, Lausanne, Sep. 1996, Nucl. Inst. & Meth. in Phys. Res. A 389 81-86. (1997). See also http://root.cern.ch/. Version used: 5.34/34.

[9] I. Efthymiopoulos. “Beam for RD51 in PPE134”, EDMS: 1005652, (2009).

[10] D. Pfeiffer *et al.* “The radiation field in the Gamma Irradiation Facility GIF++ at CERN”, *NIM-A, Vol.*866. 91-103. 0168-9002 - https://doi.org/10.1016/j.nima.2017.05.045. (2017).